Page 201, line 6, *for* oblique *read* certain oblique;
line 7, *for* anti-symmetric *read* symmetric.
Page 202, lines 26, 27, *for* anti-symmetric *read* symmetric.
Page 204, equation (17), *for* $\hat{w}'$ *read* w';
line 9, *for* $\xi = \partial u/\partial z_1 = \partial w/\partial x_1$ *read* $\xi = R(\partial u/\partial z_1 = \partial w/\partial x_1)$;
equation (19), *for* ξ_1 *read* $R\xi_1$.
Page 205, line 14, *for* $\partial w/\partial y$ *read* $\partial u/\partial y$
line 16, *for* (ii) *read* (iii);
line 16, 17, *for* respectively anti-symmetric and symmetric
read anti-symmetric;
line 17, *for* (iii) *read* (ii);
line 18, *for* respectively anti-symmetric and symmetric
read symmetric;
line 40, *for* $\chi = \frac{1}{2}(\bar{v}(\infty) - (\bar{v}^2(\infty) + 4(\lambda^2 + \mathrm{i}R(\alpha + \beta\bar{w}(\alpha/R)))^{\frac{1}{2}})$
read $\chi = \frac{1}{2}(\bar{v}(\infty) - (\bar{v}^2(\infty) + 4(\lambda^2 + \mathrm{i}R(\alpha + \beta\bar{w}(\infty)/R - \alpha c)))^{\frac{1}{2}})$.
Page 209, line 15, *for* oblique *read* certain oblique;
line15, 16, *for* anti-symmetric *read* symmetric.

Note that, corresponding to the cases (i)–(iv), the boundary conditions applicable in the blending region on $\nu_1 = z_0$ for large ν_1 are: (i) $(D+\mathrm{i}\beta)(D-\mathrm{i}\beta)v = 0$; (ii) $(D-\mathrm{i}\beta)(D+\mathrm{i}\beta)v = 0$; (iii) $(D+\mathrm{i}\beta)v = 0$; and (iv) $(D-\mathrm{i}\beta)v = 0$. Further, the anti-symmetric mode corresponding to condition (iv) with a negative value of β has similar stability characteristics to those reported for the symmetric mode corresponding to condition (iii), except that it is more stable; for example, at $z_0 = 6$ it implies a critical Reynold's number of *ca.* 76 for the anti-symmetric mode compared with 54 for the symmetric mode.

Proc. R. Soc. Lond. A **441,** 433–463 (1993)

Incremental constitutive relations for granular materials based on micromechanics

By M. M. Mehra badi, B. Loret and S. Nemat-Nasser

Figures 6 and 10 in this paper were originally printed with an incorrect layout. They are printed below, with their correct layout, complete with captions, which remain unchanged.

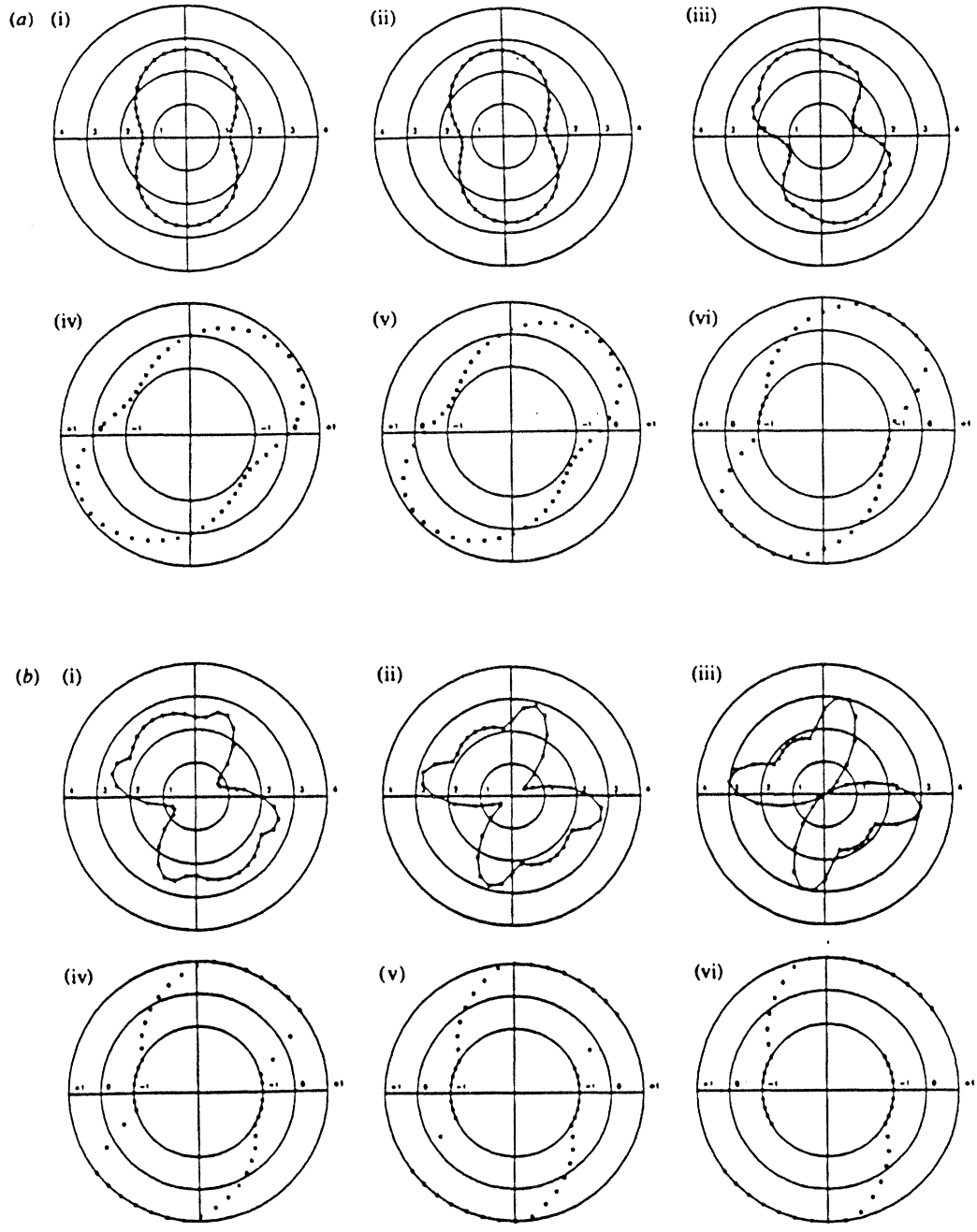

Figure 6. Distribution of magnitudes of contact forces and the directional distribution of the ratio of shear to normal forces at various increments marked on the stress–strain curve of figure 1. Increments for Mlf/p: (a) (i) 00; (ii) 05; (iii) 20; (b) (i) 30; (ii) 40; (iii) 40. Increments for $-f^{(a)}/\mu f^{(m)}$: (a) (iv) 00; (v) 05; (vi) 20; (b) (iv) 30; (v) 40; (vi) 50.

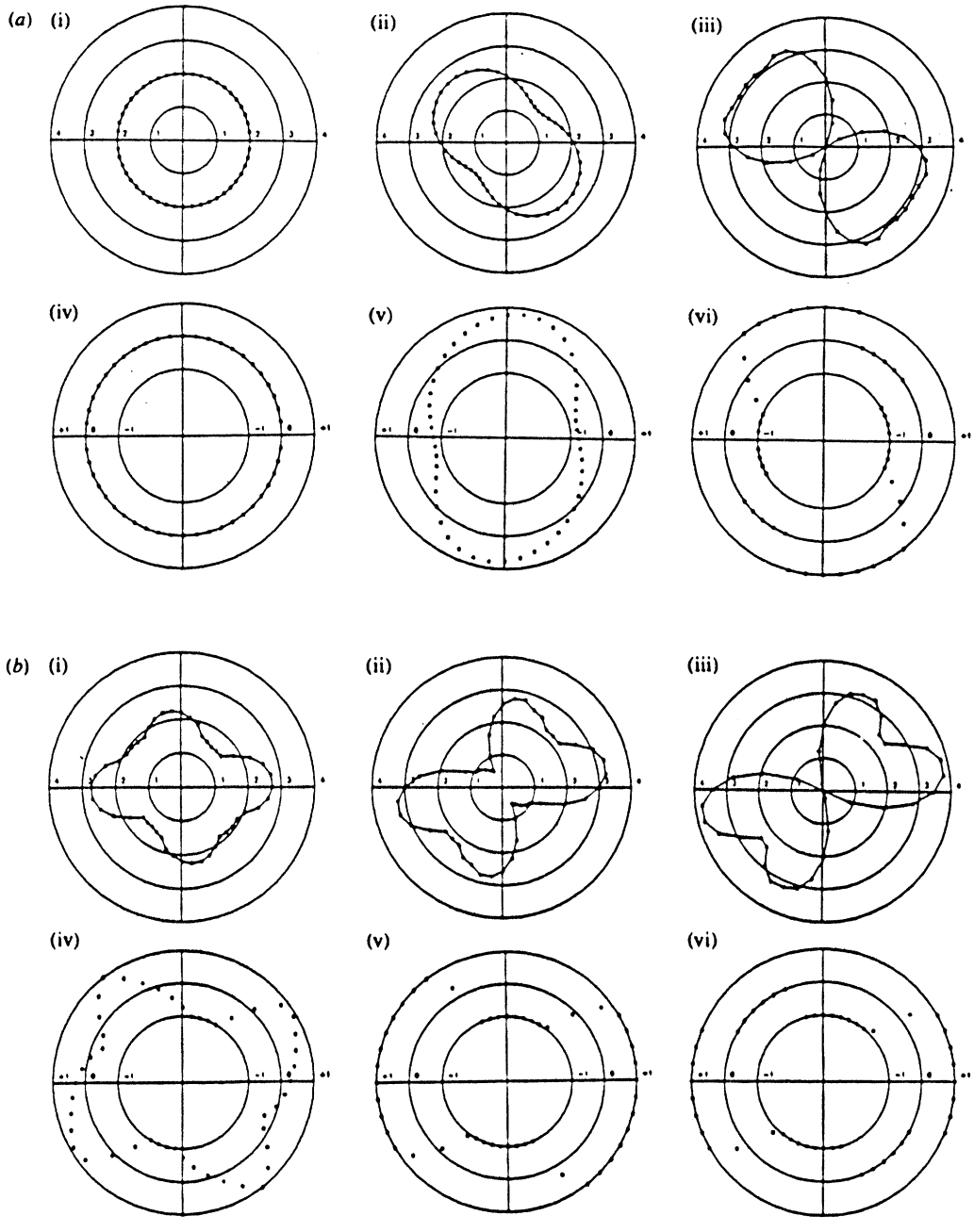

Figure 10. Distribution of magnitudes of contact forces and the directional distribution of the ratio of shear to normal forces at various increments marked on the stress–strain curve of figure 7. Increments for Mlf/p: (a) (i) 00; (ii) 05; (iii) 25; (b) (i) 39; (ii) 50; (iii) 75. Increments for $-f^{(\mathrm{s})}/\mu f^{(\mathrm{m})}$: ($a$) (iv) 00; (v) 05; (vi) 25; (b) (iv) 39; (v) 50; (vi) 75.